DE GRUYTER DOI 10.1515/htmp-2012-0084 — High Temp. Mater. Proc. 2012; 31(4-5): 479–489

Yu-ichi Uchida*, Yasuo Kishimoto, Yuji Miki and Masanori Iwase

Activities of FexO in Industrial Slags Used for External Removal of Phosphorous from Hot Metal

Abstract: In order to obtain a physicochemical knowledge of complex industrial slags, the activities of FexO in the industrial slags used for external dephosphorization of hot metal performed at practical steelmaking plants in Japan were measured by means of a solid-oxide galvanic cell in a temperature range between 1523 K and 1673 K. XRD study showed the presence of solid phases in all the slags, showing the heterogeneous character of the slags employed. With respect to the effect of CaF_2 on FexO activity, the FexO activities of the heterogeneous slags were correlated with the ratio $X(FeO)/X(CaF_2)$. High $X(FeO)/X(CaF_2)$ values corresponded to high FeO activity. This tendency is interpreted based on the phase relationship in a CaO-CaF_2-FexO ternary system. A favorable condition for external dephosphorization with less addition of CaF_2 is discussed.

Keywords: activities, FexO, phosphorous

PACS® (2010). 82.60.-s

1 Introduction

The blast furnace operators in Japan rely on supplies of relatively high phosphorus Australian iron ore, which results in a higher phosphorus input to the metal. For this reason, the problem of phosphorus removal from hot metal is more acute in Japan than in Europe or North America. This is a strong incentive for the development of a method of external dephosphorization of hot metal.

The phosphorus reaction can be expressed by:

$$2\,[P] + 5\,[O] = (P_2O_5) \tag{1}$$

External dephosphorization of hot metal is achieved by using $CaO + CaF_2 + FexO$ fluxes. Under this condition, the phosphorus reaction can be written as:

$$2\,[P] + 5\,(FexO) = (P_2O_5) + 5x\,Fe \tag{2}$$

As far as reaction (2) is concerned, a few words seem to be pertinent. For the reaction on the right hand side, it is obvious that the activity of FexO should be high and the activity of P_2O_5 should be low. It can also be noted that the rate of phosphorus removal would be controlled by the diffusion of FexO through the slag phase. This implies that the key to better control of the phosphorus levels in hot metal is a knowledge of the activities of FexO in slag. In spite of the industrial need for improved phosphorus removal, the physicochemistry of slags utilized for external dephosphorization has not been studied sufficiently, except for research by Iwase et al. [1], who investigated relatively high CaF_2-containing slags at 1673 K.

Since reaction (1) is an exothermic reaction, dephosphorization at lower temperatures is advantageous. External dephosphorization of hot metal is normally performed at approximately 1523–1673 K, which is much lower than the temperature of molten steel in the BOF. Therefore, there is a strong need for thermochemical data on this temperature range.

One objective of the present study is to measure the activities of FexO in the industrial slags used for external dephosphorization of hot metal at practical steelmaking plants in Japan by means of a solid-oxide galvanic cell [2] in a temperature range between 1523 K and 1673 K. P_2O_5 activities can be evaluated by utilizing the measured FexO activities.

Recently, among a number of components in steelmaking slags, use of fluorspar (CaF_2) has been reconsidered from the viewpoint of environmental issues. The most recognized beneficial effect of CaF_2 is lowering of the viscosity and melting temperature of slag. This makes slag more fluid and promotes equilibrium at the slag-metal interface. On the other hand, spent slags containing CaF_2 cannot generally be utilized as roadbed or landfill materials because of pollution caused by elution (leaching) of fluorine ions from the slags. For better environmental

---

***Corresponding author: Yu-ichi Uchida:** Steelmaking Research Department, Steel Research Laboratory, JFE Steel Corporation, Chiba 260-0835, Japan, E-mail: yu-uchida@jfe-steel.co.jp
Yasuo Kishimoto: Steelmaking Research Department, Steel Research Laboratory, JFE Steel Corporation, Chiba 260-0835, Japan
Yuji Miki: Steelmaking Research Department, Steel Research Laboratory, JFE Steel Corporation, Chiba 260-0835, Japan
Masanori Iwase: The late Professor, Ferrous Metallurgy Research Group, Department of Energy Science and Technology, Kyoto University, Kyoto 606-8501, Japan

control, development of flux with a reduced content of fluorspar, or even a fluorspar-free flux, is required. Therefore, obtaining thermochemical information about the effect of CaF_2 on FexO activities for industrial slags at temperatures typically used in external dephosphorization would appear to be an urgent matter.

Such thermochemical information about the effect of CaF_2 on FexO activities for complex slags has been reported by several researchers [1, 3–6]. The research by Turkdogan and Pearson [2, 3] concerned temperatures above 1800K. Iwase et al. [1] mainly studied homogeneous liquid slag. Iwase et al. [6] also reported the FexO activities of a $CaO\text{-}CaF_2\text{-}SiO_2\text{-}FeO$ quaternary system in which some slags comprised liquid and solid phases. In spite of these studies, the effect of CaF_2 on FexO activities in heterogeneous industrial slags is still unclear. Therefore, the second objective of this study is to investigate the dependence of measured FexO activities on the CaF_2 content in industrial slags.

2 Experimental procedure

2.1 Chemical analysis of slags

The slags investigated in this research were supplied by major blast furnace companies in Japan as part of a study by the "Minimization of steelmaking slag as an industrial waste" Research Group of the Iron and Steel Institute of Japan (ISIJ). All concerned wish to remain anonymous. Lumps of the slags were crushed and ground, and metallic iron was then removed magnetically from the slag powder. The compositions of the slags were determined by ICP spectrometry analysis [7] except for sulfur and fluorine, which were determined by flaming analysis [8] or wet chemical analysis [9]. Ferrous iron was also determined by wet chemical analysis [10].

2.2 XRD analysis

The slag was wrapped in a platinum plate and heated to 1673 K, which corresponds to the highest temperature in the following emf measurements, in a stream of argon. After holding for 1 hour, the slag was quenched in liquid nitrogen. The slag was then ground into powder and analyzed by XRD at room temperature for detection of solid phases.

2.3 Emf measurement

An electrochemical method incorporating zirconia as an electrolyte and an $Mo + MoO_2$ mixture as a reference electrode has been applied successfully to the determination of the FexO activities in steelmaking slags by the present authors [2]. The technique consists of charging slags in an iron crucible together with pure silver to bring the slag into equilibrium with solid iron in a stream of pure argon, and measuring the equilibrium oxygen partial pressure by means of a solid-state zirconia cell. An automatic device based on this method, which was developed by Heraeus Electro-Nite Ltd., was used in this study [11]. The electrochemical cell adopted in the equipment can be expressed as follows:

$$+)\ Mo/Mo + MoO_2/ZrO_2\ (MgO)/(FexO)_{slag} + Fe/Ag/Fe\ (-$$

The electrochemical cell consists of a zirconia tube of 3.6 mm OD, 2.2 mm ID, and 32 mm length, a $Mo + MoO_2$ mixture, and a molybdenum rod of 1 mm diameter and 200 mm length. An iron crucible of 19 mm OD, 16 mm ID, and 37.5 mm length is charged with 8 g of pure silver and 1 to 3 g of sample slag and placed on a steel pedestal. The electrical contact to the outer electrode of the zirconia cell is made via the pedestal.

The chemical potential of oxygen at the slag electrode is established by the reaction

$$x\ Fe(s) + (1/2)\ O_2 = FexO\ (in\ slag) \tag{3}$$

The open-circuit cell voltage is given by the following equation [11]

$$E = (RT/F)\ \ln[\{P_{O_2}(ref)^{1/4} + P_e^{1/4}\}/\{P_{O_2}(slag)^{1/4} + P_e^{1/4}\}] + Et \tag{4}$$

where $P_{O_2}(ref)$ is the oxygen partial pressure of the reference electrode, $Mo + MoO_2$, *i.e.*, $RT\ln\{P_{O_2}(ref)/atm\} = -576.1 + 0.1692\ (T/K)$ [12], P_e is the oxygen partial pressure at which the ionic and n-type electronic conductivities are equal, *i.e.*, $\log(P_e/atm) = 20.40 - 6.45 \times 10^4/(T/K)$ [13], and Et is thermoelectromotive force (emf) between Mo and steel, which was measured by a separate experiment. The other symbols in equation (4) have the usual meanings. The activities of FexO can be calculated by

$$a_{FexO} = [P_{O_2}(slag)/P°_{O_2}(slag)]^{1/2} \tag{5}$$

where $P°_{O_2}(slag)$ is the equilibrium oxygen partial pressure of the mixture, "pure" $FexO + Fe(s)$. The standard state for a_{FexO} is taken as either "pure" nonstoichiometric liquid

FexO, or "pure" nonstoichiometric solid FexO, in equilibrium with pure solid iron. For the former and the latter cases, $\log(P^{\circ}_{O_2}/\mathrm{atm}) = 4.39 - 2.35 \times 10^4/(T/\mathrm{K})$ [14] and $\log(P^{\circ}_{O_2}/\mathrm{atm}) = 6.71 - 2.74 \times 10^4/(T/\mathrm{K})$ [15], respectively.

3 Experimental results

3.1 Composition of the slags

Table 1 shows the chemical compositions of the slags. The compositions of these slags are significantly different from one another.

Figure 1 shows the isothermal section of the phase diagram of a $CaO\text{-}CaF_2\text{-}SiO_2$ system at 1673 K [16]. Figure 2 shows the isothermal section of the phase diagram of a $CaO\text{-}SiO_2\text{-}P_2O_5$ system at 1673 K after Matsu-suye et al. [17].

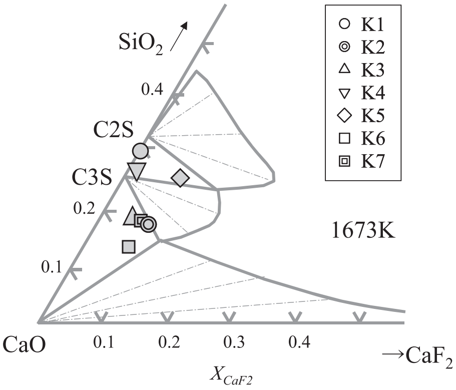

Fig. 1: Phase diagram of the $CaO\text{-}CaF_2\text{-}SiO_2$ system at 1673 K

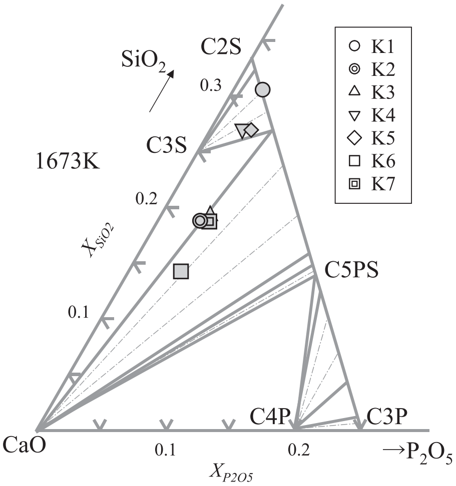

Fig. 2: Phase diagram of the $CaO\text{-}P_2O_5\text{-}SiO_2$ system at 1673 K

Code	X_{FexO}	X_{CaO}	X_{MgO}	X_{MnO}	X_{SiO_2}	$X_{P_2O_5}$	X_{CaF_2}	X_{Na_2O}	$X_{Al_2O_3}$	X_{TiO_2}	X_{CaS}	B*
K1	0.139	0.486	0.021	0.075	0.225	0.020	0.000	0.002	0.023	0.010	0.001	2.38
K2	0.043	0.614	0.043	0.019	0.151	0.027	0.078	0.001	0.015	–	0.007	3.80
K3	0.031	0.600	0.068	0.043	0.151	0.030	0.045	0.003	0.028	–	0.001	3.93
K4	0.094	0.535	0.027	0.045	0.206	0.018	0.011	0.026	0.020	0.012	0.005	2.69
K5	0.019	0.490	0.075	0.102	0.191	0.021	0.069	0.001	0.018	0.014	0.000	3.14
K6	0.080	0.611	0.052	0.023	0.108	0.031	0.059	0.003	0.016	0.008	0.010	4.94
K7	0.067	0.586	0.049	0.026	0.144	0.029	0.056	0.003	0.017	0.012	0.010	3.81

* $B = (X_{CaO} + X_{MgO} + X_{MnO})/(X_{SiO_2} + X_{P_2O_5})$

Table 1: Compositions of slags used in the external dephosphorization of hot metal

It is characteristic of this diagram that no liquidus line is present near the CaO apex.

Hereafter, the following notations are used.

$$C3S = 3CaO \cdot SiO_2 = Ca_3SiO_5$$

$$C2S = 2CaO \cdot SiO_2 = Ca_2SiO_4$$

$$C3S2 = 3CaO \cdot 2SiO_2 = Ca_3Si_2O_7$$

$$CS = CaO \cdot SiO_2 = CaSiO_3$$

$$C4P = 4CaO \cdot P_2O_5 = Ca_4P_2O_9$$

$$C3P = 3CaO \cdot P_2O_5 = Ca_3P_2O_8$$

$$C5PS = 5CaO \cdot P_2O_5 \cdot SiO_2 = Ca_5P_2SiO_{12}$$

$$\langle C3P\text{-}C2S\rangle ss = \text{Solid solution between } 3CaO \cdot P_2O_5 \text{ and } 2CaO \cdot SiO_2$$

In Figure 1, the slag compositions listed in Table 1 are expressed. Other components in the slags such as FexO, MgO, MnO and so forth were omitted in plotting the slag compositions on this diagram. As shown in the figure, the slags K2, K3, K6 and K7 may be saturated with solid CaO, and also with C3S. The slags K1, K4 and K5 may consist of liquid and solid phases in saturation with C3S and C2S.

In Figure 2, the slag compositions listed in Table 1 are also expressed in same manner as Figure 1. As shown in the figure, the slags K2, K3, K6 and K7 may be saturated with solid CaO and ⟨C3P-C2S⟩ss. The slags K1, K4 and K5 may lie in the region saturated with solid C3S and ⟨C3P-C2S⟩ss.

3.2 Presence of solid phases in the slags

All the slags employed in this study showed a set of sharp peaks due to the presence of solid phases. It is considered that the slags employed in this study consisted of liquid and solid phases at the temperature of the emf measurements. It is worth mentioning that a peak which corresponds to the possible presence of solid CaO (containing a minor amount of MgO or FeO as solid solution) was observed with the slags K2, K3, K6 and K7.

3.3 FexO activities

Table 2 lists the measured cell potential (emf). The equilibrium oxygen partial pressures and the activities of FexO are also shown in the table.

Sample Code	T (K)	E* (mV)	P_{O_2} (atm)	$a_{\langle FexO\rangle}$	$a_{(FexO)}$
K1	1526	96.2	1.29E-12	0.475	0.362
K1	1563	103.6	3.27E-12	0.464	0.379
K1	1607	108.8	1.04E-11	0.475	0.421
K1	1624	116.4	1.35E-11	0.443	0.403
K1	1677	128.3	4.17E-11	0.421	0.418
K2	1524	298.7	2.42E-15	0.021	0.016
K2	1538	303.0	3.48E-15	0.021	0.016
K2	1604	308.2	2.73E-14	0.025	0.022
K2	1643	331.2	4.71E-14	0.021	0.020
K2	1673	335.3	1.03E-13	0.022	0.022
K3	1524	209.0	3.83E-14	0.084	0.064
K3	1593	233.5	1.76E-13	0.074	0.063
K3	1604	241.5	1.96E-13	0.068	0.060
K3	1644	252.2	4.85E-13	0.066	0.062
K3	1673	262.7	8.37E-13	0.062	0.062
K4	1526	123.0	5.69E-13	0.316	0.241
K4	1538	130.3	6.70E-13	0.292	0.228
K4	1564	146.6	9.34E-13	0.245	0.201
K4	1603	159.8	2.08E-12	0.224	0.197
K4	1643	181.2	3.63E-12	0.183	0.172
K4	1674	193.0	6.23E-12	0.168	0.166
K5	1523	236.9	1.57E-14	0.055	0.041
K5	1563	258.0	3.21E-14	0.046	0.038
K5	1604	260.4	1.09E-13	0.051	0.045
K5	1643	272.1	2.64E-13	0.049	0.046
K5	1674	276.0	5.89E-13	0.052	0.051
K6	1526	172.1	1.27E-13	0.149	0.114
K6	1564	209.7	1.41E-13	0.095	0.078
K6	1603	224.4	3.14E-13	0.087	0.076
K6	1607	229.4	3.07E-13	0.082	0.072
K6	1644	230.6	9.04E-13	0.090	0.085
K6	1677	265.2	8.74E-13	0.061	0.060
K7	1523	150.4	2.23E-13	0.206	0.156
K7	1604	209.5	5.01E-13	0.108	0.095
K7	1643	217.1	1.29E-12	0.109	0.103
K7	1677	230.2	2.37E-12	0.100	0.100

* Emf values are not corrected to thermal-emf between Mo and steel. For correction, subtract Et obtained from the following equation from the values given in this table; Et (mV) = −12.4 + 0.0212 × T

Table 2: Experimental results of emf measurements

The temperature dependence of the emfs is given in Figure 3. As shown in the figure, a single straight line could be drawn through the data points for each slag, and no flexion is observed. This would indicate that, within the temperature range employed in this study, there is no drastic change in the phase relationship of each slag.

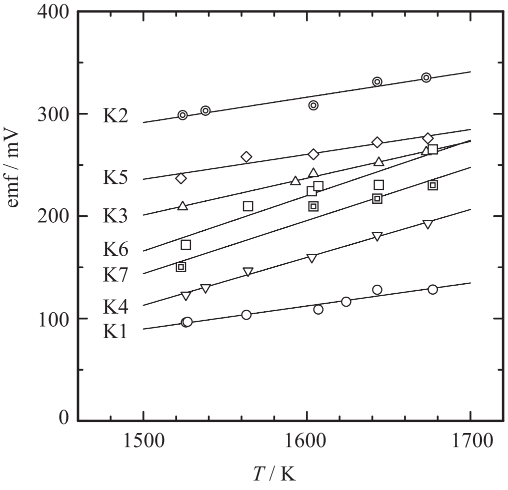

Fig. 3: Measured cell potentials (emfs) as the function of temperature

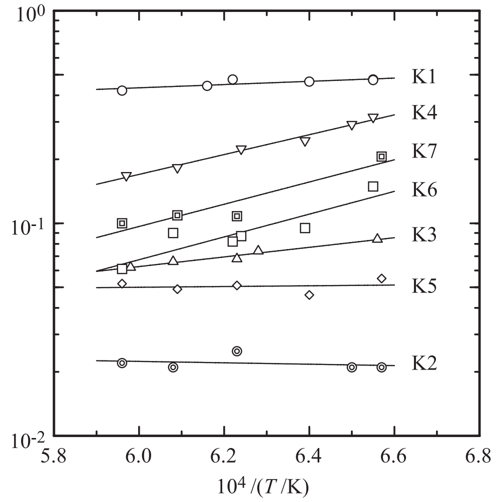

Fig. 4: Activities of FexO as the function of reciprocal temperature

The activities of FexO are shown against reciprocal temperature in Figure 4. The standard state of FexO is taken as “pure” nonstoichiometric solid FexO in equilibrium with pure solid iron. As in the case of the emfs, smooth relationships are observed between the FexO activities and the reciprocal temperature.

In the following discussion, the activity values of FexO at 1673 K are employed to analyze the dependence on slag composition. In this case, the standard state of FexO is taken as “pure” nonstoichiometric liquid FexO in equilibrium with pure solid iron.

4 Discussion

4.1 Comparison of FexO activities with the literature data

The activities of FexO determined in this study are shown in Figure 5. The solid line in the figure denotes the Raoultian relation, which corresponds to an activity coefficient of unity. The activity coefficients of FexO of the present slags are not more than 3.

Turkdogan and Pearson [4] has provided iso-activity curves for FexO in the pseudo-ternary system of (CaO + MgO + MnO)-FexO-($SiO_2 + P_2O_5$) at 1873 K. Iwase et al. [1] also drew such diagram for (CaO + MgO + MnO + CaF_2)-FexO-($SiO_2 + P_2O_5$) at 1673 K. Yamada et al. [18] gave the relation between γ_{FexO} and (mass%CaO)/(mass%SiO_2) based on industrial data at open hearth furnace and BOF. By making use of these information, values of FexO activities for the present slags can be derived. Such derived values are compared with those obtained with the emf measurements, and this is presented in Figure 6. Temperature conversion of the activity data is done under an assumption of regular solution. Rough correspondence with Iwase et al. and Yamada et al. may be shown in the figure, however, it is difficult to find a significant tendency among such data comparison. Therefore, an attention should be focused on more detailed consideration of the effect of slag composition.

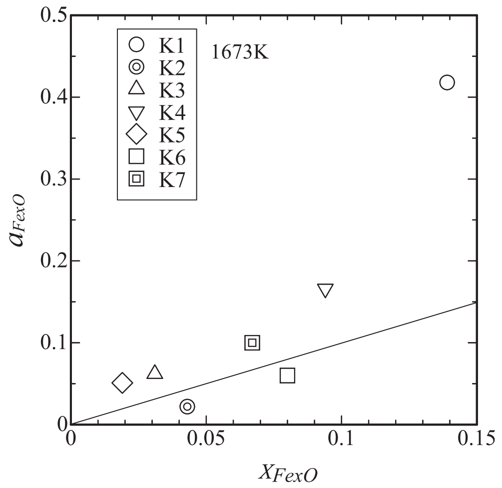

Fig. 5: Activities of FexO as the function of X_{FexO} at 1673 K

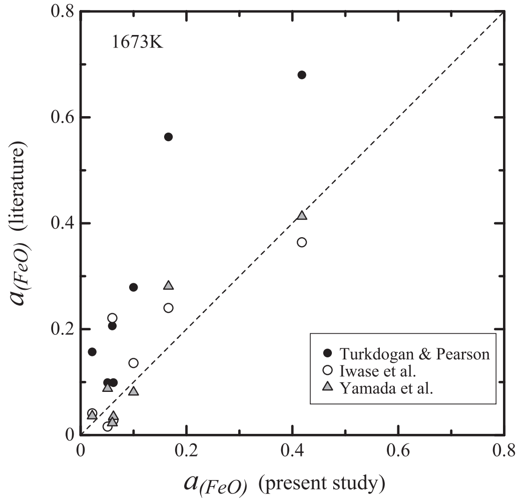

Fig. 6: Comparison between a_{FexO} in the present study and those derived from the literature.

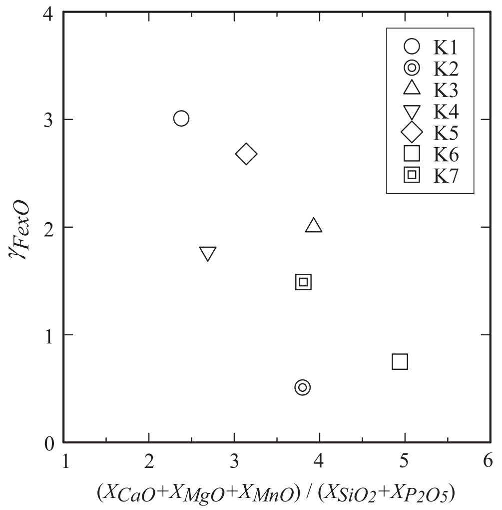

Fig. 7: Activity coefficient of FexO as the function of $(X_{CaO}+X_{MgO}+X_{MnO})/(X_{SiO_2}+X_{P_2O_5})$ at 1673 K

4.2 Dependence of FexO activities on slag composition

In Figure 7, the activity coefficients of FexO, γ_{FexO}, are given against a ratio $(X_{CaO}+X_{MgO}+X_{MnO})$ to $(X_{SiO_2}+X_{P_2O_5})$. This ratio corresponds to empirical basicity and is referred to as B in Table 1. γ_{FexO} decreases with increasing B but shows scattering near $B=4$. It is difficult to find a particular correlation among these limited data.

γ_{FexO} is shown against the mole fraction of CaF_2 in Figure 8. A slight tendency that γ_{FexO} decreases with increasing X_{CaF_2} may be observed, which might suggest some effect of CaF_2 on FexO activities.

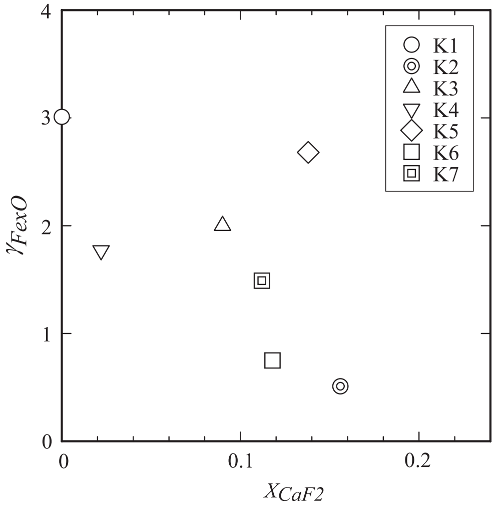

Fig. 8: Activity coefficient of FexO as the function of X_{CaF_2} at 1673 K

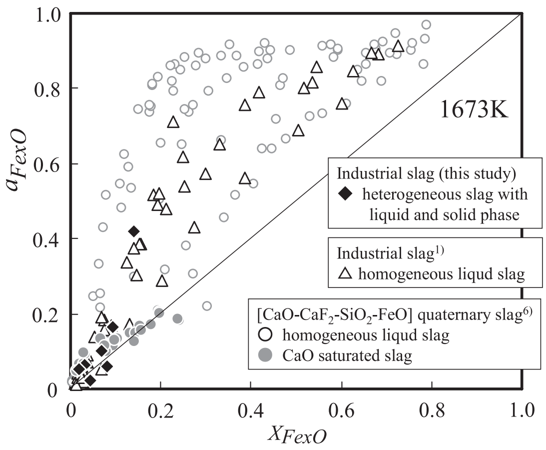

Fig. 9: Activities of FexO as the function of X_{FexO} at 1673 K

In order to obtain more comprehensive information on the effect of CaF_2 on the activities of FexO in silicate slags, the present data were compared with data in the literature. In Figure 9, the relationships between the activities of FexO and X_{FexO} in the slag containing CaF_2 are shown again, together with the data presented by Iwase et al. for industrial slags used for external dephosphorization of hot metal [1] and for CaO-CaF_2-SiO_2-FexO quaternary synthetic slags [6]. The open symbols correspond to homogeneous liquid slags, and the closed symbols correspond to slags consisting of liquid and solid phases. The FexO activities of the homogeneous liquid slags show large positive deviations from the Raoultian law. Although the slags saturated with a solid phase correspond to relatively low FexO contents, the deviation is smaller.

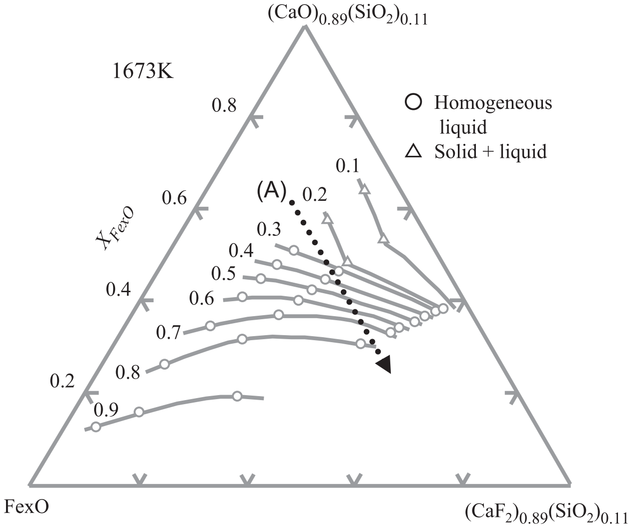

Fig. 10: Iso-activity curves for the $(CaO)_{0.89}(SiO_2)_{0.11}$-$(CaF_2)_{0.89}(SiO_2)_{0.11}$-FexO pseudo-ternary slags at 1673 K

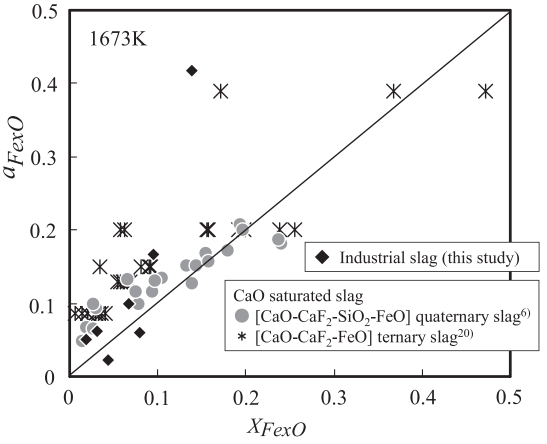

Fig. 11: Activities of FexO as the function of X_{FexO} for heterogeneous slags at 1673 K

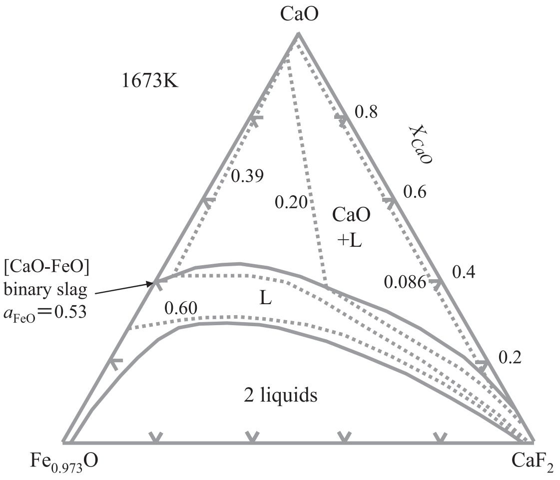

Fig. 12: Iso-activity curves for the CaO-CaF_2-FexO ternary slags at 1673 K

The effect of CaF_2 on FexO activities for silicate slags was shown by Turkdogan and Pearson [3]. Their results are based on data obtained with homogeneous liquid slags above 1800 K. Those researchers reported that the activity of ferrous oxide increases regularly with the fluoride content of the slag with fixed FeO and SiO_2 concentrations. Their result can be followed by the systematic study by Iwase et al. [6], who measured FexO activities in a CaO-CaF_2-SiO_2-FexO quaternary system and obtained iso-activity curves on the $(CaO)_{0.89}(SiO_2)_{0.11}$-$(CaF_2)_{0.89}(SiO_2)_{0.11}$-FexO pseudo-ternary diagram, as in Figure 10. Let us consider that a slag composition is changed along line (A), that is, the slag composition lies in the homogeneous liquid region and CaO is substituted for CaF_2 at a fixed FexO concentration. The activity of FexO in the slag decreases according to the iso-activity curves. The same tendency can be observed with the results after Hawkins and Davis [19] and Iwase et al. [20] for a CaO-CaF_2-FexO ternary system and Taniguchi et al. [21] for a CaO-CaF_2-Al_2O_3-FexO quaternary system.

In order to obtain a clue as to the difference in the FexO activities of complex slags comprising solid and liquid phases, the FexO activities are compared with those of synthetic slag systems, using data after Hawkins and Davis [19] for a CaO-CaF_2-FeO ternary system and after Iwase et al. [6] for a CaO-CaF_2-SiO_2-FeO quaternary system. A comparison is shown in Figure 11. The data from these previous studies were all chosen for slags saturated with solid CaO. In this figure, it is hard to find any distinct differences among the slags employed.

Let us refer to the phase diagram of a slag containing CaO, CaF_2 and FeO. Since a detailed phase diagram for a CaO-CaF_2-SiO_2-FeO quaternary system near the CaO apex is not available, the phase diagram of a CaO-CaF_2-FeO ternary system with iso-activity curves [19] as in Figure 12 is used here as reference. In the region with two-phase coexistence of solid CaO and a liquid phase, the FexO activities are decided along the conjugation line from the CaO apex. The FexO activities change along the liquidus line through change in $X(FeO)/X(CaF_2)$. High $X(FeO)/X(CaF_2)$ values corresponds to high FeO activity.

From this point of view, FeO activity data are plotted again against $X(FeO)/X(CaF_2)$ in Figure 13. In this figure, some difference appeared between each slag system, in that CaO-CaF_2-FeO ternary slags show relatively higher activity compared to those of CaO-CaF_2-SiO_2-FeO quaternary slags. The activities of industrial slags are much lower. It should be noticed at this point, that the slags K2,

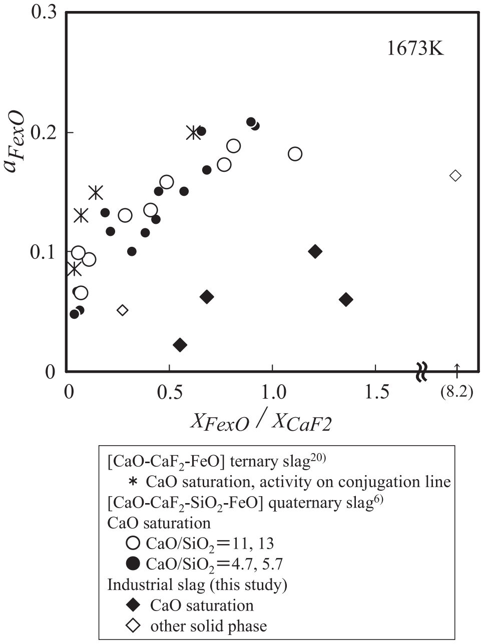

Fig. 13: Activities of FexO as the function of X_{FexO}/X_{CaF_2} for heterogeneous slags at 1673 K

K3 and K7 were recognized as CaO-saturated slags in XRD observation and have mutually similar SiO_2 contents and *B*. In this figure, slag K4 has a large *X(FeO)/X(CaF$_2$)* value and plotted at a considerable distance from the other slags in the direction of the horizontal axis. The data for slag K1 are not plotted because the value of *X(FeO)/X(CaF$_2$)* is infinity.

This difference can be understood qualitatively in terms of the liquidus composition. In Figure 12, provided an SiO_2 component is added to the ternary system and the phase relationship does not change, it would be estimated that the liquidus region is enlarged. With respect to the [CaO + L] region, as long as another silicate compound is not formed, the liquidus line would shift away from the FexO apex. This would result in a lower FexO content on the liquidus line and would possibly lead to the lower FexO activities.

In case a minor amount of another component is concerned, for example, Al_2O_3, MgO or MnO, which are common in complex steelmaking slags, the liquidus region would display further enlargement. The liquidus line would slide much closer to the CaO apex and, in turn, much further from the FexO apex. This would possibly lead to further lowering of the FexO activities.

CaF_2 would mainly be dissolved in the liquid phase. An increase in the amount of CaF_2 in the slag could lead to an increase in the volume of the liquid phase. FexO should also exist in the liquid phase, although a small amount might be included as a solid solution. Accordingly, an increase in CaF_2 content can cause dilution of FexO in the liquid phase, then lower the FexO concentration in the liquid phase and the FexO activity. This is one possible explanation for the behavior shown in Figure 13.

With the industrial slags investigated in this study, X-ray diffraction observation revealed the presence of another solid phase. Such presence of another solid phase may influence the phase relationship and FexO activity. The present authors deem, however, that the consideration presented above would not be unreasonable. As can be seen in Figure 2, the composition of slags K2, K3, K6 and K7 lie in the [CaO + ⟨C2S-C3P⟩ss] region. This means that the conjugation line is drawn from the CaO apex and the activities of the components hold on the conjugation line. This situation might respond to the above explanation, even in those complex slags.

For the slags K1, K4 and K5, the slag compositions lie in the region [C3S + C2S + L] in Figure 1 and in the region [C3S + ⟨C2S-C3P⟩ss] in Figure 2. No implication of solid CaO was found in XRD observation. Although the phase relationship is different, let us consider a possible explanation for the effect of *X(FexO)/X(CaF$_2$)* on FexO activity. Figure 14 shows a C2S-CaF_2-FexO pseudo-ternary diagram [22]. A similar diagram is also cited for CS-CaF_2-FexO in the reference. This diagram does not show a liquidus line near the C2S apex. One can find that the phase relationship in this diagram is quite similar with those in CaO-CaF_2-FexO ternary systems and could draw the liquidus line as a dotted line in the diagram by analogy with Figure 11. In the [C2S + L] region in the diagram, FexO activity would depend on the ratio *X(FeO)/X(CaF$_2$)*. In case of C3S saturation, no reliable diagram has been obtained, and

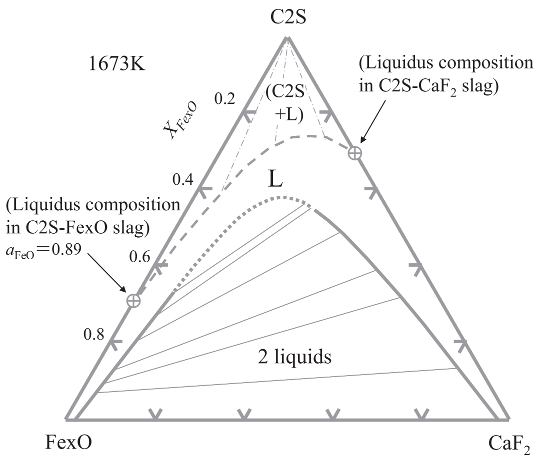

Fig. 14: Phase diagram of the C2S-CaF$_2$-FexO pseudo-ternary system at 1673 K

further research is required for the confirmation of such an explanation.

4.3 Evaluation of P_2O_5 activities

In order to calculate the P_2O_5 activity in slag based on reaction (1), the oxygen content in metal equilibrated with slag is required. At the temperatures used in external dephosphorization, i.e., 1523–1673 K, liquid iron contains carbon greater than approximately 3.5 mass%. Consequently, the oxygen contents in quenched iron cannot be determined with satisfactory accuracy.

Alternatively, the oxygen potential in the slags was measured in this study at the temperature at the final stages of external dephosphorization. It may be assumed that equilibrium had been achieved between the slag and hot metal in such final stages. In this case, the activity of P_2O_5 can be calculated by the following equation [23]

$$2\,\mathrm{P}\ (\text{in iron}) + 5/2\ \mathrm{O_2}\ (\text{in slag}) = \mathrm{P_2O_5}\ (\text{in slag}) \qquad (6)$$

$$\log(a_{\mathrm{P_2O_5}}/[a_{\mathrm{P}}{}^2\{P_{\mathrm{O_2}}(\text{slag})\}^{5/2}]) = 67380/(T/\mathrm{K}) - 28.44 \qquad (7)$$

The activities of phosphorous in hot metal a_P were calculated using the interaction parameter for phosphorous [24].

Table 3 shows the temperatures and compositions of hot metal in the final stages of external dephosphorization, which was performed with the present slags at practical steelmaking plants. The activities of P_2O_5 thus calculated are also listed in Table 3. Since external dephosphorization of hot metal with the present slags was conducted at various temperatures, it is impossible to compare the data at the same temperature. Therefore, the difference in temperature is taken into consideration by multiplying the logarithm of $a_{P_2O_5}$ by the term RT.

4.4 Favorable condition for external dephosphorization

Reduced FexO activities impede the dephosphorization reaction. On the other hand, decreased P_2O_5 activities promote the reaction. This situation may be represented as shown in Figure 15. This figure illustrates the balance of the FexO activity and the P_2O_5 activity for the industrial slags.

Reaction (2) is expressed as follows:

$$\mathrm{R}T \ln a_{\mathrm{P_2O_5}} = 5\mathrm{R}T \ln a_{\mathrm{FeO}} + 2\mathrm{R}T \ln h_{\mathrm{P}} - \Delta G^\circ(2) \qquad (8)$$

where $\Delta G^\circ(2)$ is the standard free energy change · of reaction (2) and h_P is the Henrian activity of phosphorus in hot metal.

If the phosphorus content in hot metal and the hot metal temperature are given, one can calculate lines expressing the relationship between the FexO activity and the P_2O_5 activity on Figure 15 with the slope of 5. For example, the solid line in Figure 14 shows this relation-

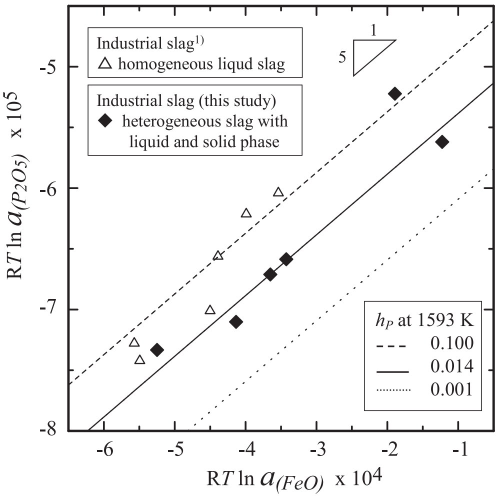

Fig. 15: Relationship between RT ln a_{FexO} and RT ln $a_{P_2O_5}$

Sample Code	Composition in mass percent					T (K)	log $a_{P_2O_5}$
	C	Mn	P	S	Si		
K1	3.6	0.1	0.015	0.009	0.01	1623	−17.77
K2	3.9	0.37	0.012	0.005	0.03	1536	−24.59
K3	3.8	0.18	0.015	0.007	Tr	1593	−21.71
K4	4.5	0.34	0.067	0.004	0.02	1538	−17.44
K5	3.84	0.35	0.01	0.002	0.01	1603	−22.85
K6	4.09	0.1	0.018	0.021	0.02	1602	−21.16

Table 3: Compositions of the hot metal in the final stages of external dephosphorization

ship at $T = 1593$ K, $h_P = 0.014$, which corresponds to slag K3. The dotted line and broken line correspond to $h_P = 0.100$ and 0.001 at the same temperature, respectively.

The present data are distributed along the solid line in the figure. This would be because temperatures and h_P for the hot metal involved in this study are typical for external dephosphorization at practical steelmaking plants in Japan, and do not differ significantly except for K4, which corresponds to a relatively higher phosphorus content in the hot metal (0.067 mass%).

The data points in the upper right side of the figure (slags K1 and K4) correspond to high FexO activity and high P_2O_5 activity. On the contrary, the data located in the lower left side (slags K2, K3, K5, K6) show low FexO activity and low P_2O_5 activity. It is worth mentioning, at this point, that the former slags contain less CaF_2 than the latter slags.

Figure 15 also shows the data for the practical steelmaking slags containing CaF_2 employed in ref. 1. The composition of the hot metal after dephosphorization with these slags and the calculated P_2O_5 activities are listed in Table 4. Since the activity measurements were conducted only at 1673 K in their study, it is noted that the FexO activities at 1673 K were employed to calculate $RT \ln a_{FexO}$. Although the industrial slags employed in this study had relatively lower contents of CaF_2 compared to the slags in ref. 1, the phosphorus level after dephosphorization is sufficiently low. Furthermore, the slags in this study show higher FexO activity if compared at a similar $RT \ln a_{P_2O_5}$ value. Reduction of CaF_2 would increase P_2O_5 activity; however, it would raise FexO activity in heterogeneous slag, as mentioned in this paper.

Now, one can find that external dephosphorization is feasible with either high FexO activities or low P_2O_5 activity. For the dephosphorization operator, it is required that the FexO activity in the slag should attain a sufficient level from the thermochemical point of view in order to keep the phosphorous content in hot metal at the present level.

$a_{(FeO)}$*	Phosphorus content in metal (mass%)	T** (K)	log $a_{(P_2O_5)}$
0.042	0.112	1548	−20.71
0.06	0.09	1548	−20.12
0.032	0.057	1548	−21.88
0.014	0.016	1548	−24.78
0.030	0.02	1573	−23.04
0.013	0.03	1543	−24.37

*) obtained at 1673 K

**) obtained at the final stages of external dephosphorization

Table 4: Activities of FeO and P_2O_5 in complex slags used for external dephosphorization of hot metal cited from ref #1

5 Conclusion

The activities of FexO in the industrial slags used for external dephosphorization of hot metal performed at practical steelmaking plants in Japan were measured by means of a solid-oxide galvanic cell in a temperature range between 1523 K and 1673 K. The results can be summarized as follows:

1. Smooth relationships are observed between the FexO activities and reciprocal temperature, which indicates that there is no drastic change in the phase relationship of each slag within the temperature range employed in this study.
2. The FexO activity in the heterogeneous slag is correlated with the ratio *X(FeO)/X(CaF_2)*. High *X(FeO)/X(CaF_2)* values correspond to high FeO activity. This tendency is interpreted based on the phase relationship in a CaO-CaF_2-FexO ternary system.
3. A favorable condition for external dephosphorization with less addition of CaF_2 is suggested to be higher FexO activity in slag.

Received: April 30, 2012. Accepted: July 11, 2012.

References

[1] M. Iwase, N. Yamada, H. Akizuki and E. Ichise, *Arch. Eisenhuttenwes.*, **55**, 10, 471–476 (1984).

[2] M. Iwase, N. Yamada, K. Nishida and E. Ichise, *Trans. Iron. Steel Soc. A.I.M.E.*, **4**, 69–75 (1984).

[3] E. T. Turkdogan and J. Pearson, *JISI*, **173**, 217–223 (1953).

[4] E. T. Turkdogan and J. Pearson, *JISI*, **176**, 59–63 (1954).

[5] H. Suito and R. Inoue, *Tetsu-to-Hagane* (in Japanese), **68**, (10), 1541–1550 (1982).

[6] M. Iwase, H. Akizuki, E. Ichise and Y. Tanaka, *Steel Research*, **57**, (9), 436–443 (1986).

[7] J. O. Burman, C. Ponter and K. Bostrom, *Anal. Chem.*, **50**, (4), 679–680 (1978).

[8] Japanese Industrial Standards, "*Methods for determination of sulfur in iron ores,*" JIS-M-8217, Japanese Standard Association, Tokyo (1990).

[9] Japanese Industrial Standards, "*Testing methods for industrial wastewater,*" JIS-K-0102, Japanese Standard Association, Tokyo (1993).

[10] Japanese Industrial Standards, "*Method for determination of ferrous oxide in iron ore,*" JIS-M-8213, Japanese Standard Association, Tokyo (1978).

[11] T. Ogura, R. Fujiwara, R. Mochizuki, Y. Kawamoto, T. Oishi and M. Iwase, *Metall. Trans. B*, **23**, 459–466 (1992).

[12] M. Iwase, M. Yasuda and T. Mori, *Electrochi. Acta.*, **193**, 261–266 (1979).

[13] M. Iwase, E. Ichise, M. Takeuchi and T. Yamasaki, *Trans. Japan Inst. Metals*, **251**, 43–52 (1984).

[14] H. Hoshino and M. Iwase, *Metall. Trans. B*, **27**, 375–378 (1996).

[15] M. Iwase, N. Yamada, E. Ichise and H. Akizuki, *Trans. Iron. Steel Soc. A.I.M.E.*, 4, 53–59 (1984).

[16] T. Watanabe, H. Fukuyama and K. Nagata, *ISIJ Int.*, **42**, (5), 489–497 (2002).

[17] M. Matsu-suye, M. Hasegawa, K. Fushi-tani and M. Iwase, *Steel Research Int.*, **78**, (6), 465–467 (2007).

[18] K. Yamada, Y. Kawai and T. kawaka, *Tetsu-to-Hagane* (in Japanese), **65**, S674 (1979).

[19] R. J. Hawkins and M. W. Davies, *JISI*, **209**, 226–230 (1971).

[20] M. Iwase, E. Ichise, N. Yamada and K. Nishida, *Trans. Iron. Steel Soc. A.I.M.E.*, **4**, 47–53 (1984).

[21] Y. Taniguchi, K. Morita and N. Sano, *ISIJ Int.*, **37**, (10), 956–961 (1997).

[22] “*Slag Atlas*,” edited by Verein Deutscer Eisenhuttenleute (VDEh), Verlag Stahleisen GmbH, Dusseldorf, Germany, Figure 3, 449 (1995).

[23] E. T. Turkdogan and J. Pearson, *JISI*, **173**, 398–401 (1953).

[24] H. Schenck and E. Steinmetz, *Wirkungsparameter von Begleitelementen flussiger Eisenlosungen und ihre gegenseitigen Beziehungen*, Verlag Stahleisen GmbH., Dusseldorf, Germany (1968).